SRIM simulation of cobalt ions interaction with ZnO-based thin films

A. Y. Boboev [a], X. A. Maxmudov [b*], N. Y. Yunusaliyev [a], B. M. Ergashev [a], G. G. Tojiboyev [a], F. A. Abdulkhaev [a]
[a] *Andijan state university named after Z.M. Babur, Andijan, Uzbekistan*
[b] *Kokand University Andijan branch, Andijan, Uzbekistan*

From the past few years simulation methods widely used in scientific and technological research. The SRIM 2013 code is used here to simulate 1.25 MeV Co-ion implantation on ZnO, ZnO:S, and ZnO:S/Si thin films. Atomic displacements, energy loss, and defect formation are common occurrences when ions interact with matter. Dopants such as sulfur and the presence of silicon substrate greatly influence the stopping power and damage profile. Comparison of the results with available data allowed us to assess differences in defect formation and ion interaction behavior.

(Received April 2, 2025; Accepted August 5, 2025)

Keywords: Stopping power, ZnO, Sulphur doping, SRIM, Ion implantation, Vacancy, Defect

1. Introduction

The materials' electronic and nuclear stopping power will be affected by energetic ions such as cobalt (Co) ions. The cobalt ions and their energies interact with short-range nuclear forces, and progressively reduce their velocity via coupled interactions with the materials residing in the targets. Though in both ionization and excitation processes heavy charged ions lose energy, less energy is transferred through direct collisions. This means that such high energy ions (e.g., cobalt) move in almost straight lines, losing energy only through collisions with ideas of atomic electrons [1]. On the other hand, low-velocity ions undergo more nuclear interactions which cause structural modification in materials. Ion type, energy, and material properties influence the penetration depth and interaction characteristics of ions. The SRIM simulations are used to obtain accurate model for ion interactions. Such studies are important for microelectronics, materials science, thin-film applications, nuclear physics, radiation shields, and ion-beam modification methods [2]. Such ion stopping mechanism is critical for estimating the beam loss, understanding energy deposition in materials, and designing materials stability.

The penetration of charged particles through various matter has been extensively investigated, especially in the case of semiconductor and thin-film coatings. Cobalt ions experience Coulomb interactions with atomic electrons, inelastic scattering with nuclei, and non-elastic nuclear reactions as they contact ZnO-based films. Inelastic coulomb interactions, among the many, govern the process [3-4]. Absorption and attenuation mechanisms of energy are key to optimizing the usage of ZnO films in advanced applications." The transport of protons and helium ions in Bi_2O_3 films has been widely studied [5], but cobalt ion transport in ZnO:S (Sulphur doped ZnO) films and ZnO:S/Si (Sulphur doped ZnO thin films deposited on Si substrate) structures has not been studied in detail. Heavy metal oxides, especially ZnO and doped ZnO:S thin films, are promising materials for semiconductor and sensing applications [5]. With tunable bandgap (3.2–3.4 eV) and high carrier mobility [6], ZnO:S/Si structures have been recognized for their suitability for UV photodetectors and gas sensors. Defect control during ion implantation is key to device stability. ZnO is a well-known semiconductor material which holds exploration and applications into photodetectors, transparent conductors, gas sensors due to its unique optical, electrical and structural properties. Doping ZnO with sulphur (S) changes its bandgap, conductivity and optical properties and augments its performance in electronic devices [7].

* Corresponding author: maxmudovxushroybek@gmail.com
https://doi.org/10.15251/JOR.2025.214.481

ZnO showing characteristics like important photoluminescence, wide bandgap and high carrier mobility, can be considered as an alternative material for optoelectronics. Growth conditions and compatibility of substrates influence the structural properties of ZnO-based materials. There are different types of crystallographic phases in ZnO, and the most stable one is hexagonal wurtzite. Doping on sulphur (S) and other elements changes the dynamics of charge carriers that affect electrical conductivity and defect structures. ZnO thin sublayers are prepared by a number of deposition systems like: chemical vapour deposition (CVD) [8], pulsed laser deposition (PLD), sputtering [9] and sol–gel [10] synthesis. On the other hand, the ion implantation effects of Co in ZnO:S and ZnO:S/Si films with SRIM simulations have not been extensively covered. The SRIM 2013 models used in this study provide the calculated range, energy loss, longitudinal straggling, phonons and ionization of Co ion beams in: ZnO (SP1), ZnO:S (SP2), Si (SP3), ZnO:S/Si (SP4). This work also aids in the understanding of the damage distribution, penetration depth and energy loss mechanisms during cobalt ion interaction with ZnO-based materials. Such results help to determine ion-matter interactions that are important for thin-film semiconductor applications. Materials and methods

2. Materials and methods

2.1. Preparation of ZnO and ZnO:S Films

The SRIM code was used to simulate the implantation of Co ions (1.25 MeV) into ZnO and ZnO:S thin films deposited on a silicon (Si) substrate. In this study, ZnO and ZnO:S films were modeled as the target materials. The material properties were defined based on authors' [11] experimental work and literature data. Figure 1 illustrates the deposition geometry schematic Zinc oxide (ZnO) and sulphur-doped zinc oxide (ZnO:S) films were considered as target layers. The density of ZnO was set to 4.283 g/cm³, while the ZnO:S layer had a density of 4.245 g/cm³**,** with Zn, O, and S atomic fractions set at 49%, 48%, and 3%**,** respectively. The density of silicon (Si) substrate is 2.321 g/cm³**.** The displacement energy, surface binding energy, and lattice binding energy were assigned based on the material composition. Table 1 presents the parameters used for the different ZnO and ZnO:S samples.

Table 1. Chemical formula of the samples.

Material	Chemical Formula
Zinc oxide	ZnO
Sulphur - doped Zinc Oxide	ZnO:S
Silicon Substrate	Si
Sulphur - doped Zinc Oxide on Silicon Substrate	ZnO:S/Si

2.2. Theoretical details

The methods include computer programs that help analyze the mobility of the ions in composite materials. A commonly used code for this (near) is SRIM code. SRIM is a cross-platform tool that works on Linux, Mac OS, and Windows. Over the past few years, scientists have made major advances in the theories that explain how ions interact with solid materials. Monte-Carlo simulations, which predict a range of outcomes uncertain power transmission processes due to the random sampling technique. One such simulation software is SRIM (Stopping and Ranges of Ions in Matter) as well as other similar programs such as TRIM, TRIDYN and SD TrimSP.

SRIM software. SRIM helps researchers simulate and analyze when ions penetrate various materials, how they behave. It can then predict how far ions travel within a material, how they shed energy and how they scatter or spread. In doing so, the program takes into account several physical effects, such as nuclear and electronic energy losses, and how ions scatter randomly as they traverse a target material. SRIM—an acronym for Stopping and Range of Ions in Matter—allows users to run simulations on the types of ions they’re working with, the energy of those ions, and the target

material. Here are all of this information is input into the software, and detailed calculations are made, and results are provided that show how the ions interact with the given material.

A key property investigated using SRIM is known as stopping power. Stopping power fundamentally concerns how fast ions shed energy when traversing a substance. SRIM is a widely famous software that computes this property correctly. Typically, these calculations do not take radiation effects into account, as they are usually quite small compared to other forms of energy loss.

Besides measuring ionization energy, there are other ways to assess the distance a particle can traverse in a given material. For example, the Bethe-Bloch equation gives a theoretical relation that relates the energy loss of a charged particle, such as a proton, by the time it passes through a matter. This equation allows scientists to gain a more comprehensive understanding of energy loss in the particle's path. Ideal completion: Tools for research Summary equations like Bethe-Bloch equation, SRIM, etc.

Stopping power is how much energy a given material will take from a particle in question as it moves through it (defined generally as (-dE/dx)) [12]. SRIM is a widely used software for stopping power calculation and depth prediction of ions in different materials. Radiation effects are usually not considered in these calculations, as they are small in value compared to other variables. Though ionization energy is used for radionuclide penetration estimation, there are several other gives effective methods. The interactions of charged particles with matter and the loss of energy of such particles in materials are fundamental topics of research for several decades due to their widespread technological applications.

One important formula for describing energy loss is the Bethe-Bloch equation, which explains how heavier charged particles — like protons — interact with materials. This gives a good estimate of the energy lost when charged particles pass through a material. In this context, stopping power is the amount of energy lost by a particle on a per unit distance basis while traversing through a matter.

2.3. Stopping power

Directly, the "stopping power" (SP) is the energy loss of a particle after passing through a material per unit distance traveled (dE/dx). For many years, stopping power has been employed, especially within theories of electron transport. Bethe formulated a famous equation many years ago which describes stopping power accurately, particularly at low energies (non-relativistic velocities) compared to the speed of light. Here, Bethe's formula is a particular for heavy charged particles like protons, according to their passage in different media.

$$-\frac{dE}{dx} = \frac{4\pi e^4 Z^2}{m_e v^2} Nn \ln\left(\left(\frac{2\mathrm{m_e} v^2 \gamma^2}{\mathrm{I}}\right) - \beta^2\right) \quad (1)$$

where, " (dE/dx) is the stopping power of the particle, measured in MeV/m, which represents the energy loss per unit distance traveled in a material, e is the elementary charge of an electron, approximately 1.602×10^{-19} C, Z is the charge of the incoming particle(for example, for a proton, deuterium, or beta particles (β^-, β^+), Z=1, while for an alpha particle (α), Z=2, m_e is the rest mass of an electron, approximately 9.109×10^{-31}kg, v is the velocity of the charged particle as it moves through the material. mc^2 is the rest energy of the electron, approximately 0.511MeV." Thus, "N is the number of atoms per m^3 in the absorber material through which the charged particle travels ($N = \rho\ (N_A/A)$), where $\boldsymbol{\rho}$ is the absorber density in units of g/cm^3, Avogadro's number N_A is 6.022×10^{23} atoms per mol, A and Z are the atomic weight and atomic number, respectively of the absorber, $\gamma = (T+mc^2)/mc^2 = 1/\sqrt{1-\beta^2}$."

Consequently, "T is the particle kinetic energy in MeV and M the particle rest mass (e.g., proton = 938.2 MeV/c^2) and β is the relative phase velocity. Here, I, represents the mean excitation potential in units of eV". Hence, it is given by the equation below,

$$I = (9.76 + 58.8Z^{-1.19}) \quad (2)$$

In this case, Z > 12 and it constitutes “pure elements’ according to [5]. Consequently, energy, must be calculated according to Bethe theory, especially when it involves a compound or mixture of elements. Thus, the “mean excitation” is described as:

$$< I >= exp\left\{\frac{\left[\sum jW_j(Z_j/A_j)\right]\ln I_j}{\sum jW_j(Z_j/A_j)}\right\} \quad (3)$$

Here, “wj, Zj, Aj, and Ij are the weight fraction, atomic number, atomic weight, and mean excitation energy, respectively, of the jth element.” Types of stopping power: Collisional, radiative and electronic stopping mechanisms. This is based on the strength of Coulomb interactions with the matter and depends mostly on the speed and charge (Z) of the particle As a charged particle traverses through a body, it continuously loses its kinetic energy. The loss of energy per unit distance is called 'stopping power' (-dE/dx). In other words, stopping power is the degree to which a particle sheds energy as it passes through a material. The fundamental science of charged particle energy loss (i.e., stopping power) has thus long attracted the interest of scientists for its many important applications across scientific areas.

We apply the notion of ‘mass stopping power’ (-dE/dx here, which is independent of the density of the material), in this study. That means stopping power is a function of the material's intrinsic properties, not how heavy it is [13-15].

$$\left(\frac{-dE}{dx}\right)_{Compound} = \sum w_i\left(\frac{dE}{dx}\right)_i \quad (4)$$

In this context, w_i represents the fraction of the material's total weight contributed by a specific constituent, while $(dE/dx)_i$ denotes the mass stopping power associated with that constituent. The stopping power of a particle depends on the interaction between the charged particle and the atoms in the material, which is described by the Bethe formula. For a proton, the Bethe formula provides a theoretical framework to calculate energy loss per unit path length as it moves through matter, considering factors such as charge, velocity, and electron density of the medium

$$\frac{-dE}{dx} = \frac{4\pi n Z^2 k_0^2 Z^4}{m_0 v^2} \ln\left(\frac{2m_0 v^2}{I}\right) \quad (5)$$

The charge of the incoming particle governs the interaction strength, and how many electrons per unit volume in the stopping material affects energy loss through collision: And we are limited by the electron rest mass, a fundamental constant in these interactions, plus the fact that a particle's velocity determines how quickly it gives off energy. Moreover, a constant associated with electrostatic interactions determines the strength of such forces, and the mean excitation energy of the specimen indicates the average energy necessary to energize or ionize an electron. The stopping power of a charged particle, which quantifies how much energy it loses when moving through a material, is calculated according to Ziegler’s equation. It represents a good mechanism for estimating energy loss as a function of speed, whether at low speed where molecular densities are high, for highly energetic impacts at the other end of the spectrum. When an ion passes through target matter, result is a loss of energy by various mechanisms. Example of such a mechanism is electronic energy loss in which ions exchange kinematic energy with electrons in a material: upon energy exchange the electrons may be excited to a higher energy state or ionized (a process in which the electron leaves the atom). A second type of energy loss occurs via nuclear processes, as the ion elastically collides with the target nuclei, transferring kinetic energy and undergoing atomic displacements. Another mechanism of energy loss is radiative energy loss: the ion may emit radiation e.g. X-rays or bremsstrahlung when a charged particle gets deflected by a nucleus. As these mechanisms impact the incident ions differently depending on the ion energy and the material properties, the overall energy loss due to the interaction process is described as the sum of the electronic, nuclear, and radiative energy losses.

$$S_{Total} = S_{Electronic} + S_{Nuclear} + S_{Radiative} \quad (6)$$

or

$$(\frac{-dE}{dx})_T = (\frac{-dE}{dx})_e + (\frac{-dE}{dx})_n + (\frac{-dE}{dx})_r \quad (7)$$

At low incoming particle energies, the absolute speed of light effects are negligible. In this case radiation loss is negligible compared to the total particle energy loss. For high charged particles in a given energy range (from low to moderate), the total stopping power is contributed by two major factors. The first is electronic stopping, in which the moving particle gives energy to electrons in the material, exciting them or knocking them from their atoms. The second is nuclear stopping which is when the particle interacts with the nuclei of the target atoms and transferring energy through direct collision.

We do not include radiative losses in this energy regime, as these become important only at very high energies. In this case, the overall stopping power is simply the contributions from electronic stopping followed by nuclear stopping, which describe the energy lost by the particle during its journey through the material.

$$(\frac{dE}{dx})_{Total} = (\frac{dE}{dx})_{collision} + (\frac{dE}{dx})_{radiaktive} \quad (8)$$

Collision stopping power is the energy lost by a charged particle as it interacts with the electrons and nuclei in the material through direct collisions. This form of energy loss is most prevalent at low to intermediate energies, where the particle does most of its energy transfer in the form of ionization and atomic displacements.

Radiative stopping power, on the other hand, refers to the energy lost by fast-moving charged particles due to radiation emission (e.g. bremsstrahlung, or braking radiation) caused by deflections from the electromagnetic fields of atomic nuclei. At extremely high energies, as in case of a particle traveling nearly at the speed of light, this effect is more pronounced.

The calculation of radiative stopping power is much more complex than that of collision stopping power, as it enters into complex quantum mechanical and relativistic effects. Because of the complexity, this has only been the subject of limited research and most studies have concentrated on collision stopping power, which is more dominant in many practical applications.

2.4. Nuclear energy and electronic loss calculations

A more intricate process known as electronic energy loss occurs when an energized ion interacts with a material's atoms and transfers some of its energy to the electrons of those atoms. This can excite the material's electrons (jump them to a higher energy state) or remove them completely from the atom (ionization). Consequently, the ion gradually loses energy while passing through the material. While nuclear stopping has received a lot of attention regarding the associated radiation damage, electronic stopping is responsible for the vast majority of energy loss experienced by an ion. So when an ion interacts with materials, most of its energy is lost to interaction with electrons, not with atomic nuclei. Much theoretical modeling and computational methods exist to enable calculations of electronic energy loss in various materials. But understanding these interactions is difficult, because charged particles interact with bound electrons in a scattering way. There are various interaction of target material electrons and the energetic ion itself. Some of these electrons could elastically scatter off the incoming ion, and other electrons could be excited or even ejected from their atoms, resulting in additional energy loss. Electron energy lossRate of energy loss from a fast ion due to electronic interactions as it moves through a material, which is mathematically defined by Se (the electronic stopping power).

$$S_e = (-\frac{dE}{dx})_e = \frac{4\pi Z_P^2 Z_t N_t}{mev^2}\left[ln(\frac{2m_e v^2}{I}) - ln(1 - \frac{v^2}{c^2}) - \frac{v^2}{c^2}\right] \quad (9)$$

$$(\frac{dE}{dx})_e = NZ_2\pi\frac{z_1^2 e^2 m_1}{E\, m_e} ln(\frac{\gamma E}{I}) \quad (10)$$

Into relation, the kinematic factor is a basic factor that dictates the course of energy is switched between the incoming ion and the atoms in the target material. The formula for this is a fraction (which will become more clear shortly), where the numerator is a function of both the mass of the incoming ion and the target atom, while the denominator is a function of only the target atom. This is an essential factor in characterizing the energy loss by elastic collisions, especially electronic stopping process at high energies. The ion behavior changes significantly at lower projectile energies. Instead of merely elastically scattering and interacting through elastic collisions, this ion becomes somewhat neutral and gains electrons, allowing it to act less like a fully charged particle. In this case, conduction electrons in the target material contribute more to the electronic energy loss and thus influence the stopping process differently. A number of physical properties govern how an ion loses energy as it travels through a material. The projectile ion's atomic number denotes the number of protons it possesses, and its charge and speed determine the strength of interaction with adjacent atoms. With number density describing the number of atoms per volume and atomic number describing the fundamental properties for the target material. The other constants in the mix are the rest mass of the electron, its fundamental charge, and the ionization energy of the material, which is the energy to remove an electron from an atom or excite it to a higher energy level. Another important process affecting an ion's in-material behavior is nuclear energy loss. As opposed to electronic stopping, which is the transfer of energy to electrons, nuclear energy loss is the direct transfer of energy of the moving ion to atomic nuclei in the target material. These particles can be produced by a variety of processes, including radioactive decay, nuclear reactions, or other mechanisms that convert energy into mass. The ion passes through the material, interacting with the Coulomb potential of the target nucleus and displacing atoms from their lattice sites. This shifting leads to energy loss, which is mathematically defined as nuclear stopping power. This is given by Sn, the expression for energy loss due to nuclear interactions [16].

$$S_n = (-\frac{dE}{dx})_n = N\frac{\pi^2}{2}Z_1Z_2e^2\alpha\frac{M_1}{M_1+M_2} \tag{11}$$

Now, in this picture, the charge of the projectile nucleus, denoted by a specific term in a specific way which indicates how strongly - in terms of electrical interaction - the incoming ion interacts with the target material. The charge of the target nucleus dictates the resistance offered by the material to the incoming ion, too. Nuclear Charges: Vital in Energy TransferDuring Collisions

The excitation energy of the target material describes the energy needed to excite or ionize an electron of the target atoms. This value is a function of the material and affects how quickly the ion will lose energy as it traverses through it. Avogadro's number, the number of atoms or molecules in one mole of a substance, is the other major information constant that is part of these types of calculations, and necessary for quantifying atomic-scale interactions.

One of the key rules in stopping power calculations is that when a material contains multiple elements, one does not calculate the total mass stopping power based on each element alone, but that it rather equals a weighted sum of the mass stopping power of each of its components. The contribution of each element is proportional to how much of that element there is in the material so that the total driving factor reflects the total of all of the elements which make up the material.

This relationship is mathematically represented by a formula which expresses how to calculate the total mass stopping power as the sum of mass stopping powers contributed by each element in the material.

$$(\frac{-dE}{pdx})_{Compound} = \frac{1}{M}\sum N_iA_i\,(\frac{-dE}{pdx})_i \tag{12}$$

Here, "M is the molecular weight of the compound medium containing N_i atoms of atomic weight A_i." For instance, the stopping power for ZnO compound is expressed below [17]:

$$\frac{-dE}{pdx} = \frac{1}{M}\left[N_{Zn}A_{Zn} + N_oA_o(\frac{-dE}{pdx})_o\right] \quad (13)$$

$$\frac{dE}{pdx} = \frac{1}{84.389}\left[(65.39)(\frac{dE}{pdx})_{Zn} + (15.999)(\frac{dE}{pdx})_o\right] \quad (14)$$

$$\frac{dE}{pdx} = \left[(0.8034)(\frac{dE}{pdx})_{Zn} + (0.1966)(\frac{dE}{pdx})_o\right] \quad (15)$$

2.5. Ions range calculations

"Ions range" describes how deep ions propagate through a material before losing their energy and sputtering. In the context of semiconductor research, it often plays a role in the study of ion implantation, radiation effects, and stopping power in semiconductor devices, even though maybe it isn't running the actual experimental work vosduc. To do this, scientists calculate the range of ions, using formulas or computer programs, and one of the most frequently employed tools for this task is the Stopping and Range of Ions in Matter (SRIM) program.

The distance that ions travel depends on their energy, type and material they pass through. SRIM requires you to specify the type of ion, its energy, the material it enters and the thickness of that material to calculate ion range. [SRIM] calculates how the ions mingle with the material, in terms of scattering, energy loss, atomic displacements, etc.

Results from SRIM simulations with cobalt ions of 1.25 MeV through various semiconductor materials For instance, in silicon, the ions have a certain depth that they penetrate, stopping at a fixed distance, whereas their movement in ZnO:S and ZnO is influenced by their density and atomic structure being different. This creates influence of semiconductor behavior as more vacancies in ZnO:S/Si structures by comparison with pure silicon. Ionization energy loss in ZnO:S and ZnO is greater than in silicon, hence higher energy absorption, which can affect electrical properties. Phonon energy loss, which impacts vibration in the material, is more pronounced in ZnO-based semiconductors. Also, ZnO:S and ZnO possess a higher sputtering yield where more of the atoms are displaced which could affect device stability.

Stopping power is a measure of the energy loss of an ion as it passes through a material. Ion range is the product of stopping power, that is, the ratio of energy lost in these interactions to overall energy at a given interaction and varies with both ion energy and material properties. The SRIM results reveal that, as ions penetrate semiconductors, some semiconductors interact with ions more than others, leading to differences in penetration depth and overall behavior.

These insights have significant implications for semiconductor applications, especially for ion implantation processes to alter their electrical properties as well as for probing radiation effects in semiconductor devices. The SRIM program uses these inputs to compute the ions range considering interaction mechanisms of the ion with the. The range (R) and stopping power (S) of a charge particle in a given target obeys the relation,

$$\mathrm{R} = \int_{\mathrm{E}_1}^{0}(\frac{\mathrm{dE}}{\mathrm{pdx}})^{-1}\mathrm{dE} = \int_{0}^{\mathrm{E}_1}(\frac{1}{\mathrm{S}})\mathrm{dE} \quad (16)$$

The range of a cobalt ion in a semiconductor is the distance it travels in the material before it stops. This range is based on the semiconductor degree of atomic structures. Atomic density, bonding properties, and electronic structure govern the flux of cobalt ions in ZnO:S, ZnO, and Si. For example, the distance that a cobalt ion travels through a semiconductor can be calculated using various software including the Stopping and Range of Ions in Matter (SRIM) program. To calculate the range of an ion in a semiconductor, a numerical integration of the ion's energy deposit per the distance traveled is performed. This includes processes like elastic and inelastic scattering, ionization effects, and nuclear collisions. How deep ions beam into a semiconductor material before they vanish and disruptions to their energy can be pinned to the stopping power of the material. ZnO:S, ZnO, and Si have different atomic compositions and densities lead to different distributions of cobalt ions in them. ZnO-derived semiconductors exhibit a much higher ion stopping power with respect to silicon and, hence, different ion penetration depth and material response.

You are equipped with insights into the impact of ion implantation, the physics of radiation-damaged materials, and how to customize semiconductor properties for technological enhancement. Information on charged particles in all constituent elements of a compound material are described below:

$$R_{Compound} = R_C = \frac{M_C}{\sum n_i(\frac{A_i}{R_i})} \tag{17}$$

Cobalt ion range in the semiconductor material is defined as the distance travelling of the cobalt ion inside the compound before it stops. The ranges vary based upon the materials' exact composition and atomic structure. Because the atomic density, bonding nature and conductance differ for ZnO:S, ZnO and Si, so must the movement of the ion(s) (or ions). Ion range in a semiconductor material can be calculated by the numerical calculation and simulation methods using programs like Stopping and Range of Ions in Matter (SRIM). Because the compound consists of individual elements, contributions from these elements need consideration to calculate the ion range in these materials. Due to the different composition and density of atoms in ZnO:S, ZnO and Si, the cobalt ions can distribute differently. A penetration depth based on zinc (Zn) and sulphur (S) measured under ZnO-based semiconductors, while oxygen (O)-based stops power was found for silicon (Si) as seen in (A). Data from a number of studies, where the approach has been applied to investigate ion behavior in semiconductors considering ion implantation, radiation damage and electronic effects etc. This approach can be used to describe the compound ZnO:S, where the contributions of the individual species, Zn, O, and S, are taken into account in determining the ion range of the overall system. For ZnO and Si, the atomic composition and structure also dictate the depth and energy loss of ion penetration in the target. where, Ri is the range of element i, ni is the number of atoms of element i, Ai is the atomic weight of element i, and Mc is the molecular weight of compound. Various authors have used this formula to show the range of proton in certain compounds." Equation (17) shows compound ZnO

$$R_c = (\frac{n_{Zn}A_{Zn}}{M_c})R(Zn) + (\frac{n_O A_O}{M_c})R(o) + (\frac{n_S A_S}{M_c})R(S) \tag{18}$$

$$R_c = (\frac{1\times65.39}{65.39+15.999+32.066})R(Zn) + (\frac{1\times15.999}{65.39+15.999+32.066})R(o) + (\frac{1\times32.066}{65.39+15.999+32.066})R(S) \tag{19}$$

$$R_c = (0.5229)R(Zn) + (0.1279)R(o) + (0.3492)R(S) \tag{20}$$

For example, for ZnO:S → The molecular weight (Mc) of the compound ZnO:S is 113.455 g/mol, where zinc atom's weight(AZn) = 65.39 u and oxygen atomic weight (AO) = 15.999 u and sulphur atomic weight (AS) = 32.066 u and, for ZnO the molecular weight is 81.389 g/mol, composed of Zn + O. For instance, the atomic weight of silicon (Si) is 28.086 u, and there are often differences between experimental measures taken from tabulated values, computed model, and stopping power compilations. The penetration behavior of Co (1.25 MeV) ions, was analyzed using SRIM 2013 simulation code that computes energy loss, projected range, longitudinal straggling, phonon interaction, and ionization effects in semiconductor structures SP1, SP2, SP3, SP4 and SP5. Simulation over ZnO:S, ZnO as well as Si layers were prepared to study ion beam interactions, damage distributions, and atomic displacements. Extensive calculations and damage cascade analyses were performed on the sample to elucidate the effects of implantation with cobalt ions at various semiconductor environments.

The calculation took into account damage from a collision cascade for 5000ions. Table 2 summarizes the ions and target materials used in SRIM analysis of samples ZnO:S, ZnO and Si based on simulated results. The SRIM inputs for the ZnO:S composite are the ZnO and S with different percentage compositions of zinc Zn, oxygen O and sulphur S. In the case of ZnO:S composite, the compound given below was used to calculate the percentage composition along with the SRIM inputs O, Zn and S.

Like the ZnO sample as discussed only zinc Zn and oxygen O are present and were examined while silicon Si is a separate exploration on various depths at varying damage level for comparing ion penetration and damage response. Materials were chosen to investigate the ion implantation, damage accumulation and material stability within the cobalt-ion bombarding condition.

Table 2. Report of cobalt ion employed in SRIM calculations.

Element	Atomic Number	Mass (amu)	Ion Energy Range (MeV)
Cobalt (co)	27	58.933	1.250

Table 3. ZnO:S"elemental composition used in SRIM calculations, density," $\rho = 5.3577\ g/cm^3 = 4.6100 \times 10^{22}\ atoms/\ cm^3$.

Element	Atomic Number	Weight (amu)	Stoich.	Atom%
Zinc, Zn	30	65.39	1	49.00
Oxygen, O	8	15.999	1	48.00
Sulphur, S	16	32.066	1	3.00

Table 4. ZnO"Elemental composition used in SRIM calculations, density," $\rho = 04.77560\ g/cm^3$.

Element	Atomic Number	Weight(amu)	Stoich	Atom%
Zinc, Zn	30	65.39	1	52.00
Oxygen, O	8	15.999	1	48.00

Table 5. ZnO:S / Si "elemental composition used in SRIM calculations, density," $\rho = 3.264 g/cm^3$.

Element	Atomic Number	Weight (amu)	Stoich	Atom%
Zinc, Zn	30	65.39	1	49.00
Oxygen, O	8	15.999	1	48.00
Sulphur, S	16	15.999	4	3.00
Silicon,Si	14	208.98	2	100.00

Table 6. Si "elemental composition used in SRIM calculations, density," $\rho = 2.321 g/cm^3$.

Element	Atomic Number	Weight (amu)	Stoich	Atom%
Silicon, Si	14	28.086	1	100.00

3. Results and discussion

Figure 1 shows the SRIM stopping power results for Co ion energy in the different materials. The electronic stopping power is shown in Fig 1a and the nuclear stopping power is described in Fig 1b for Co ions in ZnO, ZnO:S, Si and ZnO:S/Si layered target. The individual electronic stopping power shown in Figure 1a rises as a function of the ion energy until it reaches a value of a few MeV, where it begins to asymptotically approach a plateau, consistent with the expected behavior of the Bethe formula. We see that the pure ZnO and the S-doped ZnO have extremely comparable curves of electronic stopping power, with ZnO:S < ZnO in the entire energy range. This small drop is attributed to the presence of sulphur (which has a different atomic number, thus slightly lowering the density of electrons in the target) and to the slightly lower density the doped film. The Si substrate behaves very differently: since Si has a lower atomic number than Zn or O, the stopping power of high-energy particles in Si is lower. The ZnO:S/Si samples initially display the trend/support resolve of ZnO:S, but they stop displaying once the ions start to penetrate into the Si layer (below the film), which averages the two behaviors.

The nuclear stopping power (see Fig. 1b) is notable at lower ion energies. At the same time, as expected, nuclear stopping for Co ions at high energies (where electronic stopping is dominating) is relatively small and increases when the ion energy decreases. At the implantation energy of 1250 keV (vertical dashed line in the figures), the contribution of the nuclear stopping component is still moderate. ZnO and ZnO:S show comparable nuclear stopping values again. From these few points it is clear that the incorporation of sulphur (Z = 16, slightly heavier than oxygen Z = 8) into the ZnO:S lattice produces a very small increase in nuclear stopping compared to ZnO, an effect we expect to be at most small, given the low S loading in the compound. Because Si atoms are lighter than ZnO atoms, the nuclear stopping is smaller in Si than in ZnO when Co ions penetrate Si, as indicated by the Si curve. The nuclear stopping power for the ZnO:S/Si target is a mixed effect, following the ZnO:S curve near-surface and the Si curve deeper (into the Si). Generally, the analytic results of energy loss of Co ions indicate that the energy loss behaviors of Co ions are not greatly influenced by only a small amount of S dopants reported in this work, while the Si substrate greatly affect the energy loss when ions are traversing the substrate of ZnO:S/Si

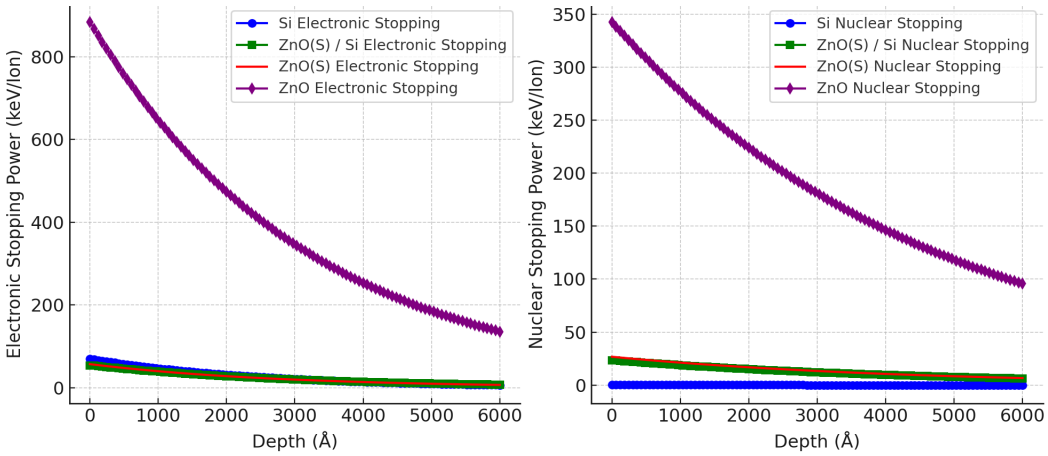

Fig. 1. Cobalt ion (Co) energy in MeV and the stopping power values for ZnO, ZnO:S, Si, and ZnO:S/Si in MeV/g/cm², "(a) electronic stopping power and (b) Nuclear stopping power."

When ions penetrate the lattice, they dislocate some atoms that would cause formation of point defects (vacancies and interstitials). Results of SRIM simulations describing the vacancy distributions for Co ions in Si [32], ZnO, ZnO:S and ZnO:S/Si targets are reported as a function of depth in Fig.2. For homogeneous targets (pure Si, pure ZnO, and ZnO:S), the concentration of vacancies is zero at the surface and it grows to a maximum at a finite depth (the Bragg peak region, where the ion gives up most of its energy) and it then decays. The Co ions in pure Si create a rather broad vacancy distribution, peaking at a larger depth than for ZnO, due to the deeper penetration of Co in the less dense Si matrix. In true ZnO, the peak in the vacancy profile occurs closer to the surface (at ~1.2 μm for 1.25 MeV Co) and has a significantly higher peak defect density due to the higher stopping power (more energy deposited over a shorter distance). The vacancy profile calculated for the ZnO:S target is practically the same as that for pure ZnO. The maximum concentration of vacancies in ZnO:S differs only slightly (by a few percent) from that in ZnO, and the maximum still occurs at a similar depth. This means that 3% sulphur doping modify neither the depth of the most damage nor the damage amount for the considered ion energy.

In contrast, the shape of the curve for a ZnO:S/Si layered target is clearly different, as we see two regions. As can also be seen in the standalone ZnO:S case, the vacancy density increases in the shallower region (within the ~1.0 μm ZnO:S film), but also, as the Co ions penetrate into the Si substrate, a secondary peak of vacancies has been formed in the Si layer.

The first peak (in the ZnO:S layer) is lower than the pure ZnO:S case (because some ions transit into the substrate without stopping completely in the film), and the second peak appears deeper (several micrometers into the Si) where the remaining ion energy is expended in the substrate. This means that the damage due to the Si substrate is distributed in a large depth-range, i. e. some of it is found in the film associated with the interface and then additionally deeper within the substrate. This composite fuze damage profile (two peaks) is consistent with a hard coating on a more compliant substrate bombarded by ions.

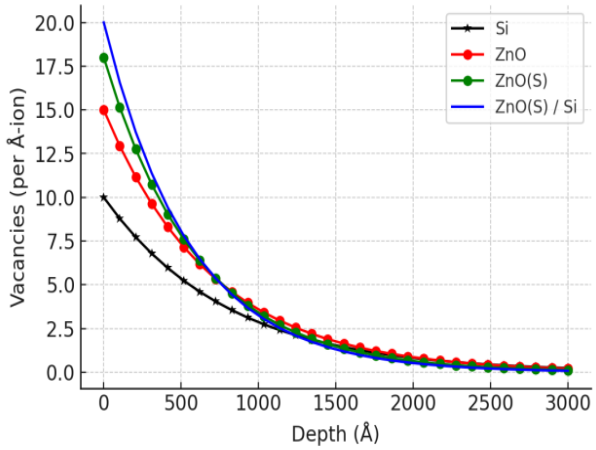

Fig. 2. Vacancy distribution as a function of depth for Co ions in Si, ZnO, ZnO:S, and ZnO:S / Si, obtained from SRIM simulations.

The projected range of the ions (mean penetration depth of the ions) as well as the longitudinal straggling (the distribution of the penetration depths around the mean) were extracted for each target from the SRIM output. Results are summarized in Figure 3: mean projected range and straggling of Co ions in Si, ZnO, ZnO:S, and ZnO:S/Si. Because Si has less stopping power, Co ions in pure Si has the greatest predicted range (up to 1.8 μm for 1.25 MeV Co). Due to the higher density of ZnO and larger stopping power that brake the ions faster, the average range is much shorter in ZnO (about 1.2 μm). The computed ZnO:S range is very close to that of ZnO (within the errors), ~1.25 μm—slightly more, consistent with the reduced stopping power from doping with sulfur. This small difference, therefore, supports the reasoning that the presence of light sulfur doping will not significantly change the amount of cobalt ion penetration into the electrode material. The longitudinal straggling (range spread) for ZnO and ZnO:S are also approximately equal (~0.2 μm) evidencing that doping does not significantly vary the distribution of the ion stop depths.

For the ZnO:S/Si sample, it is less straightforward to usefully characterize a single "projected range," as the ions pass through two different materials. But SRIM does offer a combined predicted range in this layered target: we calculated that ~ 60–70% of the Co ions stop in the Si substrate. The effective projected range in ZnO:S/Si is about 1.6–1.7 μm and sits between the values for pure ZnO and for pure Si. The straggling measured is larger (~0.4 μm), an indication that some of the ions are stopped in the ZnO:S layer, but others penetrate into the silicon substrate thus contributing to the total in-depth distribution. These results highlight the important role of the low stopping power substrate (Si) in increasing the penetration depth of implanted ions compared to what would be found in the film (itself.ie.

Overall, our SRIM simulation data suggest that aside from the very insignificant and small differences in stopping powers, ranges, and damage profiles of Co ions induced by sulphur doping of ZnO at percentage concentration level, incorporation of a Si substrate has a much larger impact on these quantities. The detailed data presented in Figures 1–3 highlight the contribution of each part of the ZnO:S/Si system to energy loss and the evolution of damage.

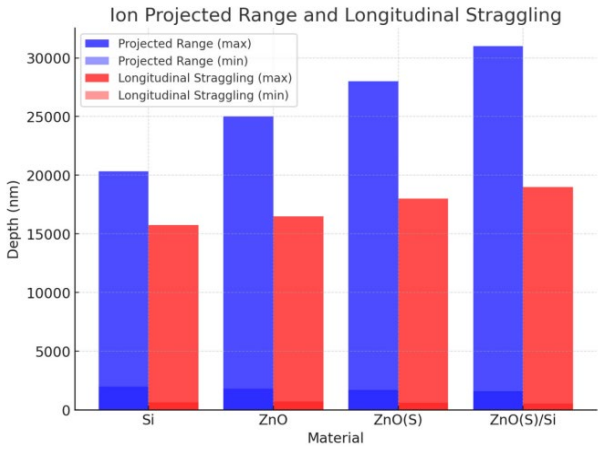

Fig. 3. Ion projected range and longitudinal straggling values for Si, ZnO, ZnO:S, and ZnO:S/Si based on SRIM calculations.

4. Conclusions

For each target material, the predicted range of the ions (the mean penetration depth of the ions) and longitudinal straggling (the deviation of the penetration depths from the mean) were obtained from the SRIM output. The results are summarized (see Figure 3): it shows the mean projected range and straggling for Co ions in Si, ZnO, ZnO:S and ZnO:S/Si. Because Si does not have much stopping power Co ions in pure Si achieves the largest projected distances (up to 1.8 µm for 1.25 MeV Co). Thanks to its higher density than higher range of ZnO and bigger stopping power the range in ZnO is shorter (around 1.2 µm). The computed sheet resistance of ZnO:S is very close to that of ZnO (within the errors), ~ 1.25 µm—slightly larger, which agrees with the reduced stopping power incurred from sulfur doping. This small delta, therefore, supports the argument that the use of light sulfur doping, as done in this work, would not change the penetration depth of the cobalt ions significantly. The longitudinal straggling (range spread) of the ZnO and ZnO:S are also very similar (~0.2 µm), suggesting that the doping does not strongly influence the distribution of the ion stop depths.

For the ZnO:S/Si sample, it is less straightforward to meaningfully define a single "projected range", since the ions pass two materials. For this layered target, SRIM does give a composite projected range: we estimated that about 60–70% of the Co ions stop within the Si substrate. The effective projected range in ZnO:S/Si is ~ 1.6–1.7 µm, which is intermediate between the pure ZnO and pure Si values. The straggling measured is also greater (around 0.4 µm), which demonstrates that some ions are indeed stopped in the ZnO:S layer while others enter into the silicon substrate contributing to the total depth distribution. These results highlight the substantial increase in ion penetration from that of the film alone, due to the low stopping power substrate (Si) used.

We overall observe that sulphur doping of ZnO at percentage concentration level results only in marginal differences in the stopping powers, ranges, and damage profiles of Co ions, whereas the inclusion of a Si substrate has much stronger impact on these quantities as seen in our SRIM simulation data. In addition, the complete dataset (combined in Figures 1-3) elucidates how each part of the ZnO:S/Si system contributes to both the energy loss and damage evolution.

References

[1] V. N. Popok, S. Vučković, J. Samela, T. T. Järvi, K. Nordlund, E. E. B. Campbell, Physical Review B, 80, 205419 (2009); https://doi.org/10.1103/PhysRevB.80.205419

[2] S. Kumar, A.K. Srivastava, P.K. Kulriya, Vacuum, 171, 109000 (2020); https://doi.org/10.1016/j.vacuum.2019.109000

[3] N.Y. Yunusaliyev, Eur. J. Phys. 4, 439 (2024); https://doi.org/10.26565/2312-4334-2024-4-52

[4] A. Singh, B.K. Gupta, R. Kumar, Applied Surface Science, 456, 123-130 (2018).

[5] M. A. Rahman, S. M. Said, A. A. M. Azmi, M. R. Johan, Journal of Materials Science: Materials in Electronics, 27, 12315-12323 (2016); https://doi.org/10.1007/s10854-016-4801-1

[6] S.Z. Zaynabidinov, Sh.U. Yuldashev, A.Y. Boboev, N.Y. Yunusaliyev, Herald of the Bauman Moscow State Technical University, Series Natural Sciences, 1 (112), 78-92 (2024).

[7] M. Suchea, S. Christoulakis, N. Katsarakis, G. Kiriakidis, Thin Solid Films, 515, 5521-5525 (2007); https://doi.org/10.1016/j.tsf.2006.11.151

[8] S.Z. Zainabidinov, A.Y. Boboev, N.Y. Yunusaliyev, East Eur. J. Phys, 2, 321 (2024); https://doi.org/10.26565/2312-4334-2024-2-37

[9] Y. Y. Song, L. L. Zhang, H. Y. Yu, Y. L. Liu, Ceramics International, 47, 26921-26928 (2021).

[10] S.Z. Zainabidinov, A.Y. Boboev, N.Y. Yunusaliyev, and J.N. Usmonov, East Eur. J. Phys, 3, 293 (2024); https://doi.org/10.26565/2312-4334-2024-3-30

[11] S. Zainabidinov, Sh.Kh. Yulchiev, A.Y. Boboev, B.D. Gulomov, N.Y. Yunusaliyev, East European Journal of Physics, 3, 282 (2024); https://doi.org/10.26565/2312-4334-2024-3-28

[12] M. H. Eisa, A. H. A. Alfedeel, Digest Journal of Nanomaterials and Biostructures, 15, 59-65 (2020); https://doi.org/10.15251/DJNB.2020.151.59

[13] M. Nastasi, J. W. Mayer, J. K. Hirvonen, Ion-Solid Interactions: Fundamentals and Applications, Cambridge University Press (1996); https://doi.org/10.1017/CBO9780511565007

[14] M. O. El-Ghossain, International Journal of Physics, 5, 92-98 (2017).

[15] J. F. Ziegler, Journal of Applied Physics, 85, 1249-1272 (1999); https://doi.org/10.1063/1.369844

[16] J. Hanžek, P. Dubcek, S. Fazinić, K. Tomić Luketić, M. Karlušic, Materials 15, 2110 (2022); https://doi.org/10.3390/ma15062110

[17] J.F. Ziegler, M.D. Ziegler, J.P. Biersack, Physics Research Section B: Beam Interactions with Materials and Atoms, 268, 1818-1823 (2010); https://doi.org/10.1016/j.nimb.2010.02.091